

Lateral buckling of beams with top bracing

Jong Sup Park†

Department of Civil Engineering, 238 Harbert Engineering Center, Auburn University,
Auburn, AL 36849-5337, USA

Young Jong Kang‡

Department of Civil and Environmental Engineering, Korea University, Seoul 136-701, Korea

(Received April 25, 2003, Accepted September 29, 2003)

Abstract. This paper presents the lateral-torsional buckling (LTB) of beams or girders with continuous lateral support at top flange. Traditional moment gradient factors (C_b) given by AISC in *LRF Specification for Structural Steel Buildings* and by AASHTO in *LRF Bridge Design Specifications* were reviewed. Finite-element method buckling analyses of doubly symmetric I-shaped beams with continuous top bracing were conducted to develop new moment gradient factors. A uniformly distributed load was applied at midheight and either or both end moments were applied at the ends of beams. The proposed solutions are simple and accurate for use by engineers to determine the LTB resistance of beams.

Key words: lateral stability; stability analysis; buckling; beam; bracing.

1. Introduction

Continuous span multigirder steel bridges are widely used in the highway bridge systems. The steel girders spans in the direction of traffic flow from bent to bent and serve as the primary load carrying members. The structural system is tied together by a reinforced concrete deck slab and transverse steel members, or diaphragms, which are connected to the girders. The top flange of the continuous girders is continuously braced against lateral or torsional movement by metal formwork during construction and in the completed bridge by the slab attached to the top flange. In this type of bridge, lateral-torsional buckling of the girders can only result from negative bending moments near the interior supports of the continuous spans.

American Association of State Highway and Transportation Officials (AASHTO) *Specifications* (Standard 1996) have required transverse diaphragms to be placed in multigirder steel bridges at a spacing not exceeding of 7.6-m (25-ft) between lines of diaphragms since 1949. A theoretical explanation for the required maximum spacing is not available. Between 1931 and 1949, diaphragms were required at a maximum spacing of 6.1-m (20-ft). With regard to recent research results of diaphragm behavior (Walker 1987, Moore *et al.* 1990, Keating and Crozier 1992,

† Post-Doctorate Fellow

‡ Professor

Azizinamini *et al.* 1994, Stallings *et al.* 1996, 1999), AASHTO *LRFD Bridge Design Specifications (LRFD Specifications, 1994)* do not have a strict requirement for diaphragms but allow the designer to use diaphragms as needed. The new AASHTO *LRFD Specifications (1998)* also do not have the mandatory 7.6-m diaphragm spacing limit.

For girders with non-composite section that do not meet the criteria set forth for width to thickness ratios and lateral bracing required for reaching the plastic moment capacity by AASHTO *LRFD Specifications (1998)*, AASHTO Equation defines the lateral-torsional buckling moment resistance of I-shaped girder as

$$M_n = 3.14EC_b \left(\frac{I_{yc}}{L_b} \right) \sqrt{0.772 \left(\frac{J}{I_{yc}} \right) + 9.87 \left(\frac{d}{L_b} \right)^2} \leq M_y \quad (1)$$

where C_b is the moment gradient modifier; I_{yc} is the moment of inertia of the compression flange about an axis in the plane of the web; L_b is the laterally unbraced length; J is the torsional constant of the beam; d is the depth of the beam; E is the modulus of elasticity of steel; M_y is the yield moment resistance of beam. Eq. (1) with $C_b = 1$ is the elastic lateral-torsional buckling resistance (M_{ocr}) for an I-shaped section under the action of constant moment in the plane of the web over the laterally unbraced length.

The C_b factor in Eq. (1) is applied to account for the effects of variable moment along an unbraced beam length. The equation for the C_b factor that has been used in many past design specifications is

$$C_b = 1.75 + 1.05 \left(\frac{M_s}{M_L} \right) + 0.3 \left(\frac{M_s}{M_L} \right)^2 \leq 2.3 \quad (2)$$

where M_s and M_L are the smaller and larger moments at the ends of the unbraced length, respectively. The ratio of M_s/M_L is taken as positive for moment causing reverse-curvature bending and negative for moment causing single-curvature bending. Eq. (2) was developed for beams with no applied loading between points of bracing. Due to this restriction, the equation is not theoretically applicable for many practical problems.

The AASHTO *LRFD specifications (1998)* and the AISC *LRFD specifications (1998)* have incorporated the following expression for C_b , which is applicable for linear and nonlinear moment diagrams

$$C_b = \frac{12.5M_{\max}}{2.5M_{\max} + 3M_A + 4M_B + 3M_C} \quad (3)$$

where M_{\max} is the maximum moment along L_b ; M_A , M_B , and M_C are the respective moments at $L_b/4$, $L_b/2$, and $3L_b/4$; and L_b is the spacing between braced points. There is no sign convention associated with Eq. (3); the absolute value is used for all moments.

Most commonly in bridge design, the unbraced length L_b in Eq. (1) is interpreted to be the distance between diaphragm lines. For this interpretation, the lateral-torsional buckling moment resistance does not account for any additional capacity provided by bracing between the ends of the segment. In multigirder steel bridges, continuous lateral or torsional bracing at top flange is provided by deck slab. Eq. (2) and Eq. (3) for C_b cannot account for continuous top flange bracing and produce very conservative estimates of lateral-torsional buckling moment resistances if top flange bracing is present.

Trahair (1979) categorized the types of continuous restraint that may act, and studied their effects on the elastic buckling of simply supported mono-symmetric beam-columns under uniform bending and axial load. Trahair (1993) also provided a summary of the various theoretical studies that have been conducted on beams with continuous braces. The general solutions provided are in many instances too complicated for design purposes, or are in graphical forms that are difficult to incorporate into design codes. *SSRC Guide* (1998) presented new moment gradient factors for beams braced at the ends and with continuous lateral bracing of the top flange. The loading is applied at the top flange that is the most detrimental case because of the increase in the torque arm as the beam buckles laterally. The proposed equation in the *SSRC Guide* (1998) includes only the effect of lateral restraint and its accuracy is not well documented.

It is, therefore, the impetus of this study to investigate numerically the lateral-torsional buckling behavior of beams with continuous top flange bracing and to develop methods for general load cases that are analogous to current lateral-torsional buckling solutions (C_b method) used in the design of beams. The numerical tools used in this study are a commercially available finite-element program MSC/NASTRAN (1998), and a graphical package MSC/PATRAN (2000). Finite-element models with uniformly distributed loading at midheight and moments at ends include only the effect of lateral restraint and conservatively neglect torsional restraint provided by concrete deck slab. First, comparisons between solution from Trahair study (1979) and FEM results of beams with continuously lateral top flange bracing under uniform moment are considered to evaluate the finite element model appropriateness. Second, FEM results for the LTB moment resistances of beams subjected to uniformly distributed load at midheight and moments at either or both ends were used to develop new moment gradient factors using the ratio of the length of bottom flange in compression to the unbraced length of the beam, L_{cb}/L_b .

2. Finite element modeling

Kirby and Nethercot (1979) were able to show in their book, *Design for Structural Stability*, that the ratio of the LTB capacity of an I-shaped beam to that of a box section beam changes as the ratio of the length to the depth of the beam changes. Therefore, the effect of the ratio of the length to the depth of the beam was considered. Although a number of cross sections and load cases were considered in the finite element model verification study, the results described here focus on three load cases and one cross section ($W33 \times 169$). Fig. 1 shows three basic simple span cases: beams subjected to uniform bending, beams subjected to only one concentrated load at the center of beam, and beams subjected to uniformly distributed load along entire span. The loading was applied at midheight of the cross section. Table 1 and Table 2 show the analytical results of these load cases and comparisons of FEM results to values from the *SSRC Guide* (1998) or *AASHTO LRFD Specifications* (1998), Eq. (3). These tables present a good agreement between the *SSRC Guide* and FEM results in the range of L_b/d from 20 to 40.

The critical moment resistance of beams with continuous lateral top flange bracing under uniform bending can be obtained by using Trahair's solution (1979). A comparison between Trahair solution and FEM results under uniform bending was also conducted to verify the finite element models used in this study. Five rolled I-shaped beams with different ratios of unbraced length to depth, L_b/d , were considered. The FEM models consist of 6 four-node plate elements through the depth of the web and 2 elements across each flange. At the ends of the unbraced length, the beam was free to

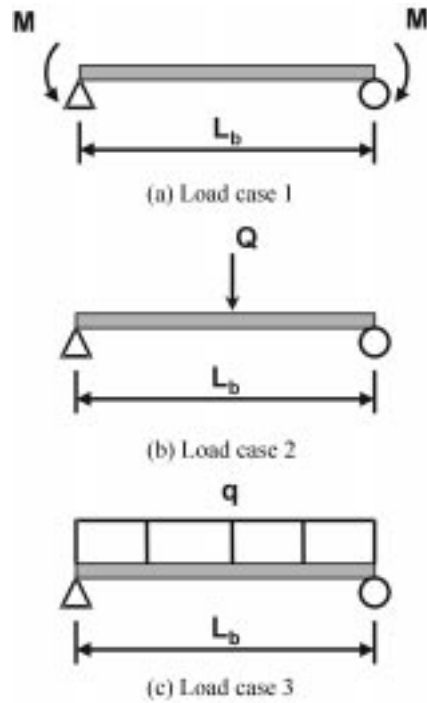


Fig. 1 Three load cases on simple span beams

Table 1 Analytical results of three basic load cases

L_b (m) (1)	L_b/d (2)	C_b		
		Case 1 (3)	Case 2 (4)	Case 3 (5)
12.2	14.19	1.00	1.304	1.137
15.2	17.74	1.00	1.330	1.138
25.9	30.16	1.00	1.350	1.135
36.6	42.58	1.00	1.350	1.131

1 ft = 0.3048 m

Table 2 Comparisons of moment gradient modifier C_b

(1)	SSRC Guide (1998) (2)	AASHTO LFRD Specification (1998) (Eq. 3) (3)	FEM Results ($L_b/d = 30.16$) (4)
Case 1	1.00	1.00	1.00
Case 2	1.35	1.32	1.35
Case 3	1.12	1.14	1.13

warp. The critical moments of these beams under uniform bending are presented in Table 3. Table 3 shows that the LTB moments from FEM analyses are in very good agreement with the values from the Trahair’s solution.

Although there are a variety of finite elements available in MSC/NASTRAN (1998), only QUAD4 is used throughout the FEM analyses because of its simple yet numerically stable performance. So, the full three-dimensional configuration of the cross-section using QUAD4 elements was considered. Three load types shown in Fig. 2 were considered to investigate the lateral-torsional buckling of beams with continuous lateral top flange bracing. Fig. 2 also shows the moment diagrams of these three load types. The typical buckling mode shapes of beams with continuous lateral top flange bracing are shown in Fig. 3. The models of Fig. 3 are subjected to uniformly distributed load and two negative end moments. Since the second eigenvalue of each model is meaningless, only first eigenvalue needs to obtain critical moment.

Table 3 Comparisons between Trahair’s Solution (1979) and FEM Results

Cross Section (1)	h/t_w (2)	L_b/d (3)	Critical Moment (kN-m)		
			Trahair Solution (4)	FEM Results (5)	Diff. (%) (6)
W30 × 477	19.2	42	12593	12176	3.3
W30 × 391	22.6	20	8947	8550	4.4
W36 × 230	45.6	40	1210	1218	0.7
W36 × 135	57.9	20	480	479	0.3
W40 × 149	59.3	38	309	320	3.5

1 ft = 0.3048 m, 1 kip = 4.45 kN, 1 kip-ft = 1.356 kN-m

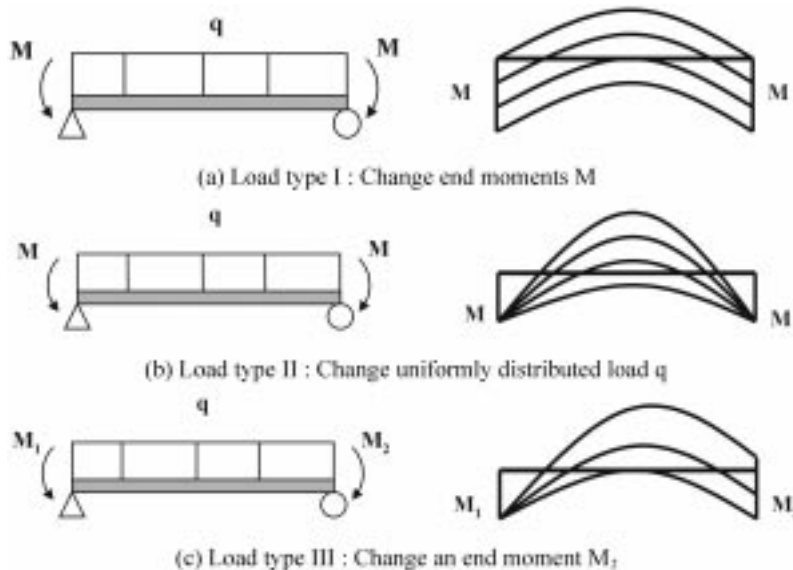


Fig. 2 Three load types and moment diagrams

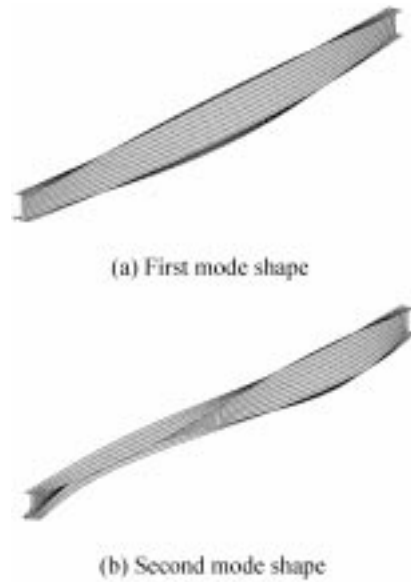


Fig. 3 Typical buckling mode shapes of beams with top bracing

3. Finite-element method results and design recommendations

FEM results for five beams subjected to 54 load cases are considered here. From the results of the finite element investigation, it was found that LTB resistance of a beam with continuous top flange bracing can be characterized by the ratio of length of bottom flange in compression to the unbraced length, L_{cb}/L_b . This ratio of lengths is also used to plot the results because it is a convenient way to summarize results for various applied loading cases. Two types of design equations were developed for beams with midheight loading. One of them is as below:

$$M_{cr} = C_{b1}M_{ocr} \quad (4)$$

In which

$$C_{b1} = -2.86\left(\frac{L_{cb}}{L_b}\right) + 7.86 \quad 0.3 \leq \frac{L_{cb}}{L_b} \leq 1.0$$

$$C_{b1} = 200\left(\frac{L_{cb}}{L_b}\right)^2 - 110\left(\frac{L_{cb}}{L_b}\right) + 22 \quad 0.15 \leq \frac{L_{cb}}{L_b} < 0.3 \quad (5)$$

where L_{cb} is the length of bottom flange in compression; L_b is the unbraced length; M_{ocr} is the LTB moment of beams in uniform bending as presented in Eq. (1) with C_b of 1; M_{cr} is the LTB moment of beams with continuously lateral bracing at the top flange subjected to a uniformly distributed load and end moments.

FEM results for load type I, load type II, and load type III are shown in Figs. 4(a), (b), and (c), respectively. The graphs show plots of the critical moment ratio, M_{cr}/M_{ocr} , versus the ratio of L_{cb}/L_b . Figs. 4(a) and (b) for load type I and type II show that the ratio of M_{cr}/M_{ocr} increases as the ratio of

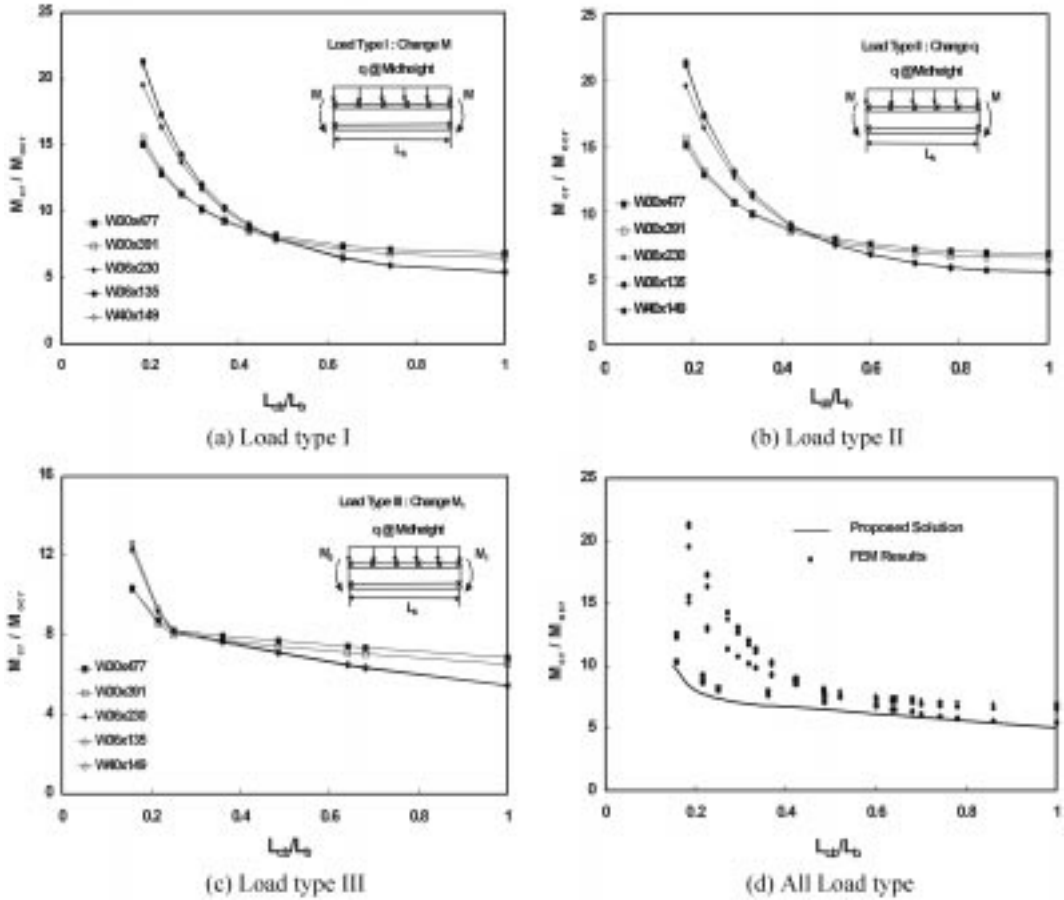


Fig. 4 FEM results and proposed solution for C_{b1}

h/t_w increases in the range of less than $L_{cb}/L_b = 0.5$. Fig. 4(c) for load type III also shows that the ratio of M_{cr}/M_{ocr} increases as the ratio of h/t_w increases in the range of less than $L_{cb}/L_b = 0.25$. Moreover, the ratio of M_{cr}/M_{ocr} increases as the warping resistance C_w/J of the beams increases.

Fig. 4(d) shows comparison between the FEM results and the proposed equations for all load types. As shown in Fig. 4(d), although the predictions from Eq. (4) are very conservative for smaller values of L_{cb}/L_b , Eq. (4) produces reasonable estimate of the C_{b1} values with respect to the finite element method results for all ranges of L_{cb}/L_b . The use of Eq. (5) should be limited for beams with $0.15 \leq L_{cb}/L_b < 1.0$. For beams with L_{cb}/L_b less than 0.15, C_{b1} must be taken as very high values, and as a results, the LTB moment in this range should not control the flexural strength of these beams.

The other new design equation for LTB behavior of beams subjected to distributed load at midheight and end moments was developed as:

$$M_{cr} = C_{b2}C_bM_{ocr} \tag{6}$$

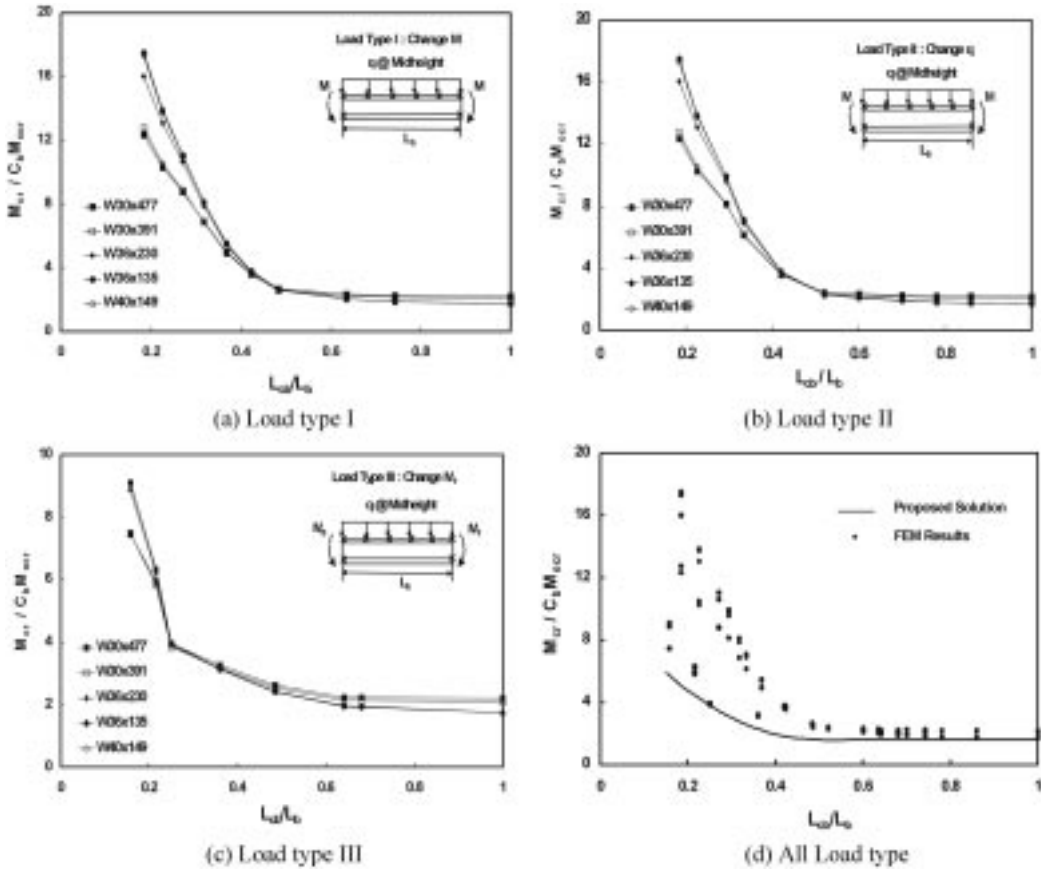


Fig. 5 FEM results and proposed solution for C_{b2}

in which

$$C_{b2} = 1.6 \quad 0.5 \leq \frac{L_{cb}}{L_b} \leq 1.0$$

$$C_{b2} = 35.2 \left(\frac{L_{cb}}{L_b} \right)^2 - 35.2 \left(\frac{L_{cb}}{L_b} \right) + 10.4 \quad 0.15 \leq \frac{L_{cb}}{L_b} < 0.5 \quad (7)$$

where the definition of L_{cb} , L_b , M_{ocr} , and M_{cr} are the same as in Eq. (4) and Eq. (5); C_b is the traditional moment gradient factor as presented Eq. (3). Therefore, a lateral-torsional buckling moment resistance of a steel beam with continuous lateral top flange bracing can be obtained multiplying proposed Eq. (7) for C_{b2} by LTB moment resistance, M_n , from Eq. (1).

FEM results for load type I, type II, and type III are shown in Fig. 5(a), (b), and (c), respectively. Fig. 5(d) is a graph for all these load types. Fig. 5(d) shows that LTB capacities of these beams would be calculated by 1.6 times than the values from Eq. (1) in the range of $0.5 \leq L_{cb}/L_b \leq 1.0$, and that the proposed solution produces somewhat conservative values for some cases (relatively stocky beam) in range of $0.15 \leq L_{cb}/L_b \leq 0.5$. Fig. 5(d) indicates that the equations for C_{b2} can be used conservatively for beam design to calculate the LTB capacity of a beam.

3. Applications

Existing continuous multispan bridges shown in Fig. 6 were considered to investigate the C_b equations. Fig. 6 shows beam details and applied loading. Model I and model II of Fig. 6 are interior spans of continuous beams so that these models have a negative end moment at each end and a uniformly distributed load. Model III of Fig. 6 is a end span of a continuous beam so that these model has a negative end moment at one end and a uniformly distributed load. Table 4 shows each cross-section property of all models.

Table 5 presents comparisons between the LTB moment resistances from the design equations and the FEM results for the continuous multispan bridges of Fig. 6. The beam models are free to warp at

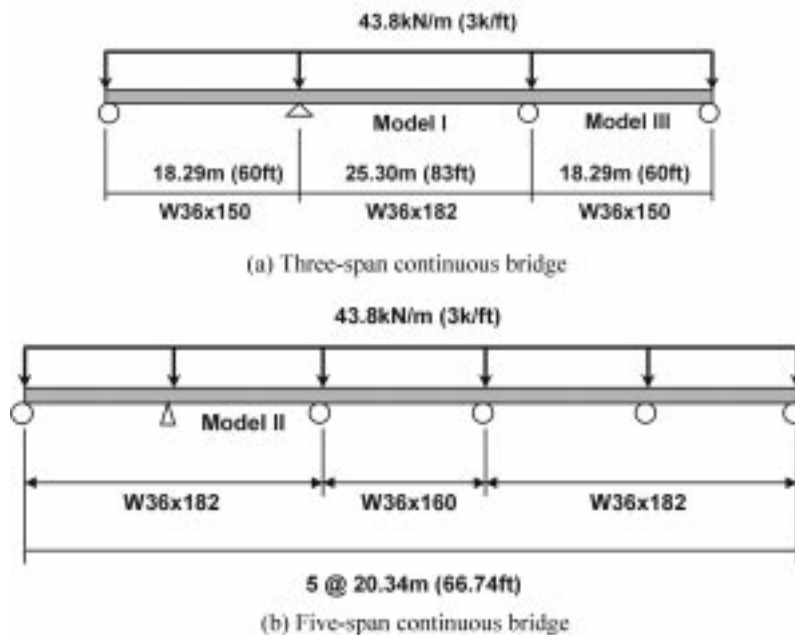


Fig. 6 Beam details for applications

Table 4 Cross-section properties in the existing multispan bridge

Section (1)	Web		Flange	
	Depth (d) (cm) (2)	Thickness (t_w) (cm) (3)	Width (b_f) (cm) (4)	Thickness (t_f) (cm) (5)
W36 × 150	91.06	1.59	30.42	2.39
W36 × 160	91.47	1.65	30.48	2.59
W36 × 182	92.28	1.84	30.67	3.00

1 in. = 2.54 cm

Table 5 Comparisons between FEM results and design equation

Model (1)	M_{ocr} (kN-m) (2)	Moment Gradient Modifier (3)	Bracing (4)	M_{cr} (kN-m)		Diff. (%) (8)
				Design Eq. (6)	FEM (7)	
I	541	$C_b^{Eq.(2)} = 1.0$	Ends	541	1088	50.3
		$C_b^{Eq.(3)} = 1.95$	Ends	1055	1088	3.0
		$C_{b1} = 6.78$	Continuous	3668	5226	29.8
		$C_b^{Eq.(3)} C_{b2} = 4.17$	Continuous	2256	5226	56.8
II	697	$C_b^{Eq.(2)} = 1.13$	Ends	788	2792	71.8
		$C_b^{Eq.(3)} = 3.03$	Ends	2111	2792	24.4
		$C_{b1} = 6.48$	Continuous	4517	5462	17.3
		$C_b^{Eq.(3)} C_{b2} = 4.88$	Continuous	3401	5462	37.7
III	538	$C_b^{Eq.(2)} = 1.75$	Ends	942	1604	41.3
		$C_b^{Eq.(3)} = 2.31$	Ends	1243	1604	22.5
		$C_{b1} = 6.94$	Continuous	3734	4023	7.1
		$C_b^{Eq.(3)} C_{b2} = 7.18$	Continuous	3863	4023	3.9

1 ft = 0.3048 m, 1 kip = 4.45 kN, 1 kip-ft = 1.356 kN-m

the ends of the unbraced length. The last column of Table 5 is the difference percentage between the results from several equations for C_b presented in previous section, and the results of finite element models having each loading and constraint condition of design equations. As shown in this table, the $C_b^{Eq.(2)}$ equation for simply supported beams produces very conservative values for all these cases, and the $C_b^{Eq.(3)}$ equation in the current AISC and AASHTO *LRFD Specifications* gives reasonably conservative values. The C_{b1} and C_{b2} equations proposed in this study for beams with continuous lateral top bracing subjected to midheight loading provide conservative values; in particular, the $C_b C_{b2}$ equation gives more conservative value than the C_{b1} equation. These two new equations can be used to obtain the LTB moment resistance of beams with continuous lateral top bracing.

4. Conclusions

Lateral-torsional buckling resistance of beams was found to be dramatically increased by providing continuous bracing along the length. It was shown that the LTB resistance of beams with continuous bracing depended upon the ratio of the length of bottom flange in compression to the unbraced length, L_{cb}/L_b . Two types of design equations for beams with midheight loading were proposed using the ratio of L_{cb}/L_b . The proposed equations indicated that the LTB capacity of a beam is improved significantly by continuous lateral bracing, especially, in the range of L_{cb}/L_b less than 0.3. The critical moment can be estimated as approximately 1.6 times the nominal moment based on LTB capacity, M_n , from current AASHTO *LRFD specifications* (1998) in the range of $0.5 \leq L_{cb}/L_b \leq 1.0$. The proposed solutions are simple and accurate for use by designers to determine the LTB resistance of beams.

References

- American Association of State Highway and Transportation Officials (AASHTO) (1994), *LRFD Bridge Design Specifications*, First Edition, Washington, D.C.
- American Association of State Highway and Transportation Officials (AASHTO) (1998), *LRFD Bridge Design Specifications*, Second Edition, Washington, D.C.
- American Association of State Highway and Transportation Officials (AASHTO) (1996), *Standard Specifications for Highway Bridges*, Sixteenth, Washington, D.C.
- American Institute of Steel Construction (AISC) (1998), *Load and Resistance Factor Design*, Second Edition, Chicago, Illinois.
- Azizinamini, A., Kathol, S. and Beacham, M.W. (1994), "Steel girder bridge design: can it be simplified", *Modern Steel Construction*, **34**(9), 44-47.
- Guide to Stability Design Criteria for Metal Structures*, 5th Ed. (1998), T.V. Galambos, ed., John Wiley & Sons, Inc. New York, N.Y.
- Keating, P.B. and Crozier, A.R. (1992), "Evaluation and repair of fatigue damage to Midland County bridges", *Report TX-92/1313-1F*, Texas Transportation Institute, Texas A&M University, College Station, Tex.
- Kirby, P.A. and Nethercot, D.A. (1979), *Design for Structural Stability*, Wiley, New York, NY.
- Moore, M., Strand, K.A., Grubb, M.A. and Cayes, L.R. (1990), "Wheel-load distribution results from the AISI-FHWA model bridge study", *Transportation Research Report 1275*, Transportation Research Board, National Research Council, Washington, D.C., 34-44.
- MSC/NASTRAN (1998), *Quick Reference Guide*, Version 70.5, the MacNeal-Schwindler Corporation, Los Angeles, CA.
- Nethercot, D.A. and Rockey, K.C. (1972), "A unified approach to the elastic lateral buckling of beams", *AISC Engineering Journal*, **9**(3), 96-107.
- Stallings, J.M., Cousins, T.E. and Stafford, T.E. (1996), "Effect of removing diaphragms from a steel girder bridge", *Transportation Research Record 1541*, Transportation Research Board, NRC, Washington, D.C., 183-188.
- Stallings, J.M., Cousins, T.E. and Tedesco, J.W. (1999), "Removal of diaphragms from three-span steel girder bridge", *J. Bridge Engineering*, ASCE, **4**(1), 63-70.
- Trahair, N.S. (1979), "Elastic lateral buckling of continuously restrained beam-columns", *The Profession of a Civil Engineer*, Sydney University Press, Sydney, 61-73.
- Trahair, N.S. (1993), *Flexural-Torsional Buckling of Structures*, CRC Press, Boca Raton, Fla.
- Walker, W.H. (1987), "Lateral load distribution in multigirder bridges", *Engineering Journal*, First Quarter, 21-28.

Appendix I. Example problems

Determine the critical moment resistances of the continuous beam spans shown in Fig. 7. All beams are of A36 steel ($F_y = 36$ ksi).

(1) Center Span

$$M_p = 2156 \text{ k-ft for } W36 \times 182 > M_{\max} = 1579 \text{ k-ft}$$

$$M_{\max} = 1579 \text{ k-ft, } M_A = 359 \text{ k-ft, } M_B = 1005 \text{ k-ft, } M_C = 359 \text{ k-ft,}$$

$$L_b = 83 \text{ ft, } L_b/h = 30, L_{cb}/L_b = 2(15.62)/83 = 0.376$$

$$M_{ocr} = 3.14E \left(\frac{I_{yc}}{L_b} \right) \sqrt{0.772 \left(\frac{J}{I_{yc}} \right) + 9.87 \left(\frac{d}{L_b} \right)^2} = 399 \text{ k-ft for } W36 \times 182 \text{ with } L_b = 83 \text{ ft}$$

$$C_{b1} = -2.86 \left(\frac{L_{cb}}{L_b} \right) + 7.86 = 6.78$$

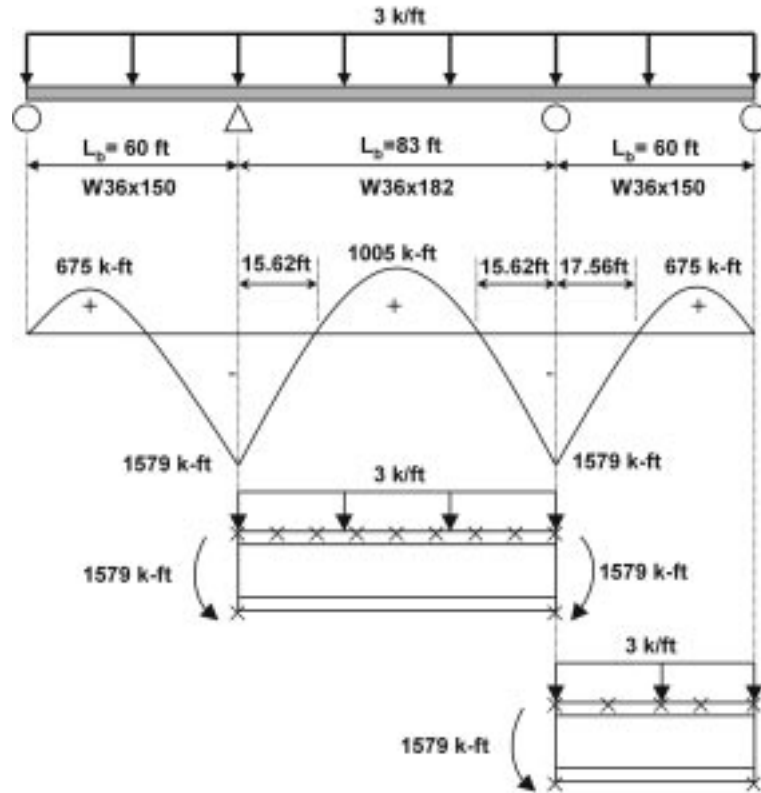


Fig. 7 Three-span continuous bridge for example

$$C_{b2} = 35.2 \left(\frac{L_{cb}}{L_b} \right)^2 - 35.2 \left(\frac{L_{cb}}{L_b} \right) + 10.4 = 2.14$$

$$C_b = \frac{12.5 M_{\max}}{2.5 M_{\max} + 3 M_A + 4 M_B + 3 M_C} = 1.95$$

$$M_{cr} = C_{b1} M_{ocr} = (6.78) (399) = 2705 \text{ k-ft} > M_{\max} = 1579 \text{ k-ft}$$

$$\text{Or } M_{cr} = C_{b2} C_b M_{ocr} = (2.14) (1.95) (399) = 1664 \text{ k-ft} > M_{\max} = 1579 \text{ k-ft} \quad \therefore \text{O.K.}$$

(2) End Span

$$M_p = 1744 \text{ k-ft for } W36 \times 150 > M_{\max} = 1579 \text{ k-ft}$$

$$M_{\max} = 1579 \text{ k-ft, } M_A = 172 \text{ k-ft, } M_B = 561 \text{ k-ft, } M_C = 618 \text{ k-ft,}$$

$$L_b = 60 \text{ ft, } L_b/h = 20.63, L_{cb}/L_b = 17.56/60 = 0.293$$

$$M_{ocr} = 3.14 E \left(\frac{I_{yc}}{L_b} \right) \sqrt{0.772 \left(\frac{J}{I_{yc}} \right) + 9.87 \left(\frac{d}{L_b} \right)^2} = 397 \text{ k-ft for } W36 \times 150 \text{ with } L_b = 60 \text{ ft}$$

$$C_{b1} = -2.86 \left(\frac{L_{cb}}{L_b} \right) + 7.86 = 6.94$$

$$C_{b2} = 35.2 \left(\frac{L_{cb}}{L_b} \right)^2 - 35.2 \left(\frac{L_{cb}}{L_b} \right) + 10.4 = 3.11$$

$$C_b = \frac{12.5M_{\max}}{2.5M_{\max} + 3M_A + 4M_B + 3M_C} = 2.31$$

$$M_{cr} = C_{b1}M_{ocr} = (6.94)(397) = 2755 \text{ k-ft} > M_{\max} = 1579 \text{ k-ft}$$

$$\text{Or } M_{cr} = C_{b2}C_bM_{ocr} = (3.11)(2.31)(397) = 2852 \text{ k-ft} > M_{\max} = 1579 \text{ k-ft} \quad \therefore \text{O.K.}$$

Appendix II. Notation

The following symbols are used in this paper:

$C_b, C_{b1}, \text{ and } C_{b2}$: modifier for moment gradient;
d	: depth of a beam;
E	: modulus of elasticity of steel;
I_{yc}	: moment of inertia of the compression flange about an axis in the plane of the web;
J	: torsional constant for a section;
L_b	: laterally unbraced length;
L_{cb}	: length of bottom flange in compression;
M_A	: absolute value of moment at quarter point of the unbraced beam segment;
M_B	: absolute value of moment at centerline of the unbraced beam segment;
M_C	: absolute value of moment at three-quarter point of the unbraced beam segment;
M_{cr}	: lateral torsional buckling strength of beam with general loading condition;
M_L	: larger moments at the ends of the unbraced length;
M_{\max}	: absolute value of maximum moment in the unbraced beam segment;
M_n	: nominal moment based on lateral-torsional buckling resistance;
M_{ocr}	: lateral torsional buckling strength of beam under constant moment;
M_S	: smaller moments at the ends of the unbraced length;
M_y	: yield moment resistance of beam.